

Normalizations are not what you think; Explicit Scale Simulation in ALDEx2

Gregory B. Gloor¹

Michelle Pistner Nixon²

Justin D. Silverman^{2,3,4}

July 24, 2024

¹ Department of Biochemistry, University of Western Ontario ² College of Information Sciences and Technology, Pennsylvania State University ³ Department of Medicine, Pennsylvania State University ⁴ Institute for Computational and Data Science, Pennsylvania State University

Abstract

In high-throughput sequencing (HTS) studies, sample-to-sample variation in sequencing depth is driven by technical factors, and not by variation in the scale (e.g., total size, microbial load, or total gene expression) of the underlying biological systems. Typically a statistical normalization is used to remove unwanted technical variation in the data or the parameters of the model to enable analyses that are sensitive to scale; e.g., differential abundance and differential expression analyses. Recently we showed that all normalizations make implicit assumptions about the unmeasured system scale and that errors in these assumptions can lead to dramatic increases in false positive and false negative rates. Here we describe updates to the ALDEx2 R package that mitigate these problems by directly modeling uncertainty in the unmeasured system scale through the use of a *scale model*. Scale models generalize the idea of normalizations and can be thought of as explicitly modeling the error in normalization by examining a distribution over all possible normalizations. Beyond enhancing the robustness of HTS analyses, the use of scale models within ALDEx2 enhances the transparency and reproducibility of analyses by making implicit normalizing assumptions an explicit part of the model building process.

Introduction

High-throughput sequencing (HTS) is a ubiquitous tool used to explore many biological phenomenon such as gene expression (single-cell sequencing, RNA-sequencing, meta-transcriptomics), microbial community composition (16S rRNA gene sequencing, shotgun metagenomics) and differential enzyme activity (selex, CRISPR killing). HTS proceeds by taking a sample from the environment, making a library, multiplexing (merging) multiple libraries together, and then applying a sample of the multiplexed library to the flow cell. Each of these steps is a compositional sampling step as only a fixed-size subsample of nucleic acid is carried over to subsequent steps. Thus, with each sampling step the connection between the size of the sampled DNA pool and the scale (e.g., size, microbial load, or total gene expression) of the measured biological system is degraded or lost. Increasingly, researchers are turning to modified experimental protocols (e.g., DNA spike-ins or cell counting) in an attempt to recover the lost biological variation in scale; see for example (1, 2). However, these protocols often do not recover meaningful biological variation but instead recover scale variation at the intermediate step in the sample preparation protocol where the DNA spike-in was added. In short, the disconnect between sample-to-sample variation in sequencing depth and biological variation in scale remains an outstanding challenge.

The analysis of HTS data suffers from several known problems that can be traced, in whole or in part, to misspecification of scale. The first issue is poor control of the false discovery rate (FDR) [(3);(4);Nearing:2022aa;@Li:2022aa], exhibited as dataset-dependent FDR control. The FDR problem is connected to the double-filtering approach that is often used, but which is known not to have appropriate FDR control (5, 6). The second issue is poor performance when analyzing asymmetric data; data that arises because of a bias in the direction of change. This type of data frequently arises in in-vitro selection experiments (SELEX),

transcriptome analysis, and microbiome analysis (7). The third issue is that these problems become more pronounced as more samples are collected; that is, more information results in a worsening of the accuracy of the analysis (9). The final problem is that these data are relative data, i.e. compositional (10, 11), and substantial effort has been put into removing this constraint.

The first three problems were recently shown by Nixon and Silverman (8) to be a result of a mismatch between the underlying size or scale of the system and the assumptions of the normalizations used for the analysis of HTS. Biological variation in scale often represents an important unmeasured confounder in HTS analyses (12). For example, cells transformed by the cMyc oncogene have about 3 times the amount of mRNA and about twice the rRNA content than non-transformed cells (13), and this dramatically skews transcriptome analysis (14). In addition, wild-type and mutant strains of cell lines, yeast or bacteria have different growth rates and RNA contents under different conditions, which affect our ability to identify truly differentially abundant genes (15–17). As another example, the total bacterial load of the vaginal microbiome differs by 1-2 orders of magnitude in absolute abundance between the healthy and bacterial vaginosis states (18), and the composition between these states is dramatically different (19, 20). Thus, a full description of any of these systems includes both relative change (composition) and absolute abundance (scale). Current methods access only the compositional information yet make implicit assumptions about the scale.

Recently, Nixon et al. (8) showed that the challenge of non-biological variation in sequencing depth be viewed as a problem of partially-identified models. They showed that *all* normalizations make some assumption about scale. These implicit assumptions are often difficult to interpret, and different normalizations provide different outputs when applied to the same dataset (3, 21–24). Intuitively, normalizations in widespread use assume that either all samples have the same scale, e.g. proportions, rarefaction (25), RPKM (26, 27), etc; or that a subset of features in one sample can be chosen as a reference to which the others are scaled e.g. the TMM (28), or LVHA (7) or the additive log-ratio (29); or that different sub-parts of each sample maintain a constant scale across samples e.g. the RLE (30); or that the geometric mean of the parts is appropriate e.g. the CLR and its derivatives.

The original ALDEx2 (31) model unwittingly made a strict assumption about scale through the CLR normalization (8). While this assumption could be useful in many cases it could never be exactly true, and others have shown that it is not always the best option (32). Nixon et al. (8) showed that better scale assumptions resulted in more reproducible data analysis including better control of both false positive and false negative results. In essence ALDEx2 has been modified to explicitly model the scale over a range of reasonable normalization parameters. Here, we briefly introduce these modifications and then show how scale uncertainty can greatly improve modeling in transcriptome and meta-transcriptome datasets to provide more robust and reproducible results.

Implementation

To be concrete, we let \mathbf{Y} denote the *measured* $D \times N$ matrix of sequence counts with elements \mathbf{Y}_{dn} indicating the number of measured DNA molecules mapping to feature d (e.g., a taxon or gene) in sample n . Likewise, we can denote \mathbf{W} as the *true* amount of class d in the biological system from which sample n was obtained. We can think of \mathbf{W} as consisting of two parts, the scale \mathbf{W}^\perp (e.g., totals) and the composition \mathbf{W}^{\parallel} (i.e., proportions). That is, \mathbf{W}^\perp is a N -vector with elements $\mathbf{W}_n^\perp = \sum_d \mathbf{W}_{dn}$ while \mathbf{W}^{\parallel} is a $D \times N$ matrix with elements $\mathbf{W}_{dn}^{\parallel} = \mathbf{W}_{dn}/\mathbf{W}_n^\perp$. Note that with these definitions \mathbf{W} can be written as the element-wise combination of scale and composition: $\mathbf{W}_{dn} = \mathbf{W}_{dn}^{\parallel} \mathbf{W}_n^\perp$.

All the normalizations in current use are data transformations that can be stated as ratios of the form $\hat{\mathbf{W}}_{dn} = \mathbf{Y}_{dn}/f(\mathbf{Y})$, where the denominator is determined by some function of the observation. We use the $\hat{\mathbf{W}}$ notation to indicate that the normalization is attempting to provide an estimate of the true value. The technical variation in sequencing depth ($\mathbf{Y}_n^\perp = \sum_d \mathbf{Y}_{dn}$) implies that observed data \mathbf{Y} provides us with information about the system composition \mathbf{W}^{\parallel} but little to no information in the system scale \mathbf{W}^\perp (Lovell et al. 2011).

Adding Scale Uncertainty in ALDEx2

The ALDEx2 R package (31, 33) is a general purpose toolbox for Bayesian modeling of HTS data. For brevity, we discuss ALDEx2 in its simplest form as a tool for estimating the magnitude and statistical significance of Log-Fold-Changes (LFC) (e.g., differential abundance or differential expression analysis), but note that it can be used to fit more complex linear models. At a high-level, ALDEx2 involves three steps: 1) a Bayesian model is used to estimate $\hat{\mathbf{W}}^{\parallel}$ given observations \mathbf{Y} ; 2) a normalization is used to estimate $\hat{\mathbf{W}}$ given the estimate $\hat{\mathbf{W}}^{\parallel}$; 3) the $\hat{\mathbf{W}}$ estimates are used to estimate LFC as part of differential abundance (or expression) analyses. For more details on ALDEx2 see (8, 31).

By default, ALDEx2 uses the CLR normalization which can be written as $\log \hat{\mathbf{W}}_{dn} = \log(\hat{\mathbf{W}}_{dn}^{\parallel}/G_n)$ where G_n denotes the geometric mean of the vector $(\hat{W}_{1n}^{\parallel}, \dots, \hat{W}_{Dn}^{\parallel})$. The CLR normalization equates to an implicit assumption that $\hat{\mathbf{W}}_n^{\perp} = 1/G_n$ (8) and even slight errors in this assumption introduces bias into the LFC estimate that is not accounted for when estimating uncertainty (e.g., confidence intervals or credible sets). In fact, Nixon et al. (8) showed that the only way in which the ALDEx2 model, or any normalization-based model, could ever be calibrated (e.g., control Type-I Error rates) was if this assumption was exactly true. In support of this assertion it is known that false discovery rates vary widely by analysis, dataset, and normalization method (34, 35). To fix this, Nixon et al. (8) showed that models should incorporate potential error in the assumptions implied by normalizations.

Nixon et al. (2023) generalized the concept of normalizations by introducing the concept of a *scale model* to account for potential error. Scale models can be incorporated into ALDEx2, turning the ALDEx2 model into a specialized type of statistical model which they called a *Scale Simulation Random Variable* (SSRV). They did this by including a model for $\hat{\mathbf{W}}_n^{\perp}$. Since the CLR normalization makes the assumption $\hat{\mathbf{W}}_n^{\perp} = 1/G_n$, the CLR normalization can be generalized by considering probability models for the scale $\hat{\mathbf{W}}_n^{\perp}$ that have mean $1/G_n$. For example, the following scale model generalizes the CLR:

$$\log \hat{\mathbf{W}}_n^{\perp} = -\log G_n + \Lambda x_n \quad \Lambda \sim N(0, \gamma^2)$$

where γ is a tunable parameter drawn from a Gaussian distribution that controls the degree of uncertainty in the CLR assumption and x_n denotes a binary condition indicator (e.g., $x_n = 1$ denotes case and $x_n = 0$ denotes control). We have made those modifications a permanent fixture of ALDEx2 which now represents the first software package designed for SSRV-based inference.

Results

Adding scale uncertainty replaces the need for dual significance cutoffs.

It is standard practice in many fields of HTS, but especially transcriptomics, to use the dual cutoff approach graphically exemplified by volcano plots (36, 37) because not all statistically significant differences are biologically relevant. Paraphrasing this we can say that in some types of datasets more samples leads to a majority of features being statistically significant. A detailed reasoning for this using modelled data is explained in two reports by Nixon et al. (8, 9), which shows that scaled models completely address this analytic issue.

We use the data of Gierliński et al. (38) who conducted a highly replicated yeast transcriptome experiment comparing a wild-type strain with a snf2 gene knockout, Δ snf2. This dataset has been used to argue that a dual cutoff approach is appropriate to limit the number of significant parts and for purposes of reproducibility (37). However, in this benchmarking study, the number of significantly different transcripts varied between 65% to >80% of all transcripts depending on the tool; in essence the desired behavior was that almost all transcripts were significantly different. The guidance on reproducibility runs counter to standard statistical practice where power is intrinsically linked to sample size and very large sample sizes are indeed desired (39). Furthermore, the dual-cutoff approach is known not to provide appropriate FDR control (5, 6). Schurch et al. (37) further suggested that different tools might be better in some conditions or datasets than others

because each tool has different intrinsic statistical power and Type 1 and Type 2 errors. Through the lens of scale uncertainty, the behaviour of the tools in this study show unacknowledged bias; false confidence in the precision of the estimate as sample size increases because of mis-specification in the scale of the data. This certainty is driven by the assumptions of the tool not the actual experiment being investigated (9).

Using either DESeq2 or ALDEx2, a majority of transcripts are statistically significantly different between groups with a Benjamini-Hochberg (40) false discovery rate (FDR) of 0.05; i.e. 4636 (79%, DESeq2) or 4172 (71%, ALDEx2) of the 5891 transcripts. Such large numbers of significant transcripts seems biologically unrealistic and furthermore breaks the necessary assumption made by the normalization methods that the majority of the features must be invariant. That 118 transcripts are identified by ALDEx2 and not DESeq2, while DESeq2 identifies 582 transcripts that ALDEx2 does not, suggests that the choice of normalization plays a role in which results are returned as significant and that some if not the majority are driven by technical differences in the analysis (22, 23, 37, 41, 42).

The effect plots (43) in Figure 1A (ALDEx2) and Supplementary Figure 1 (DESeq2) shows that the majority of significant transcripts (red, orange) have negligible differences between groups and very low dispersion and we suggest that this is driven by the experimental design (37). Scale uncertainty can be incorporated using the `gamma` parameter that controls the amount uncertainty added to the CLR mean assumption when we call either `aldex()`, or `aldex.clr()`. Figure 1B shows that setting $\gamma = 0.5$ results in far fewer transcripts being significant (205) and we observe that the minimum dispersion increases from 0.12 (unscaled) to 0.67 (scaled). The Volcano plots in Figure 1 C and D show a similar story. Here we can see that adding scale increases the minimum FDR value and increases the concordance between the FDR value and the difference between groups (compare panels C and D).

As shown by the effect plot in Figure 1 the root cause of the many statistically significant positive transcripts is the very large number of transcripts with negligible variance. This phenomenon is not unique to ALDEx2 as Supplementary Figure 1 shows that the same phenomenon occurs in DESeq2 (and presumably other methods although the relevant parameters are not exposed). This issue is not unique to this dataset and it is common practice to use a dual-cutoff by choosing transcripts based on thresholds for both corrected p-values and fold-changes (37) (here set at $\pm 2^{1.4}$ for the latter), although considerable variation in cutoff values is observed. These limits are shown by the dashed grey lines. Here, applying a dual-cutoff using a heuristic of at least a $2^{1.4}$ fold change reduces the number of significant outputs to 193 for DESeq2 and to 186 for ALDEx2, and is in-line with that observed with that found by ALDEx2 with $\gamma = 0.5$ which identifies 205. Indeed, Supplementary Figure 2, shows that even adding a very small amount of scale $\gamma = 0.1$ reduces the number of significant transcripts by more than half and the `aldex.scaleSim()` function can be used to identify those transcripts that are significant only because of an absence of scale. These results begs the question: why bother with significance tests at all if all transcripts with > 1.4 -fold expression change are statistically significant?

The effect on dispersion with increasing amounts of scale are shown in Figure 2A, where we can see that the dispersion increases as scale is added. Note that the dispersion in the unscaled data in Figure 2A reaches a minimum near the mid-point of the distribution, and also does so when the analysis is conducted with DESeq2 (Supplementary Figure 3). This shows more clearly that dispersion of many transcripts is almost negligible in the absence of scale and makes the counter-intuitive suggestion that the variance in expression of the majority of genes with moderate expression is more predictable than highly-expressed genes or of housekeeping genes (44). This is at odds with the known biology of cells where single cell counting of highly-expressed transcripts shows that they have little intrinsic variation (45).

Adding scale by setting $\gamma = 0.5$, or $\gamma = 1.0$, increases the minimum dispersion as shown in Figure 2A by the red and blue data points, and by the colored lines of fit through the centre of mass of the data. Less obvious is that the scaled dispersion estimates are rotated. Figure 2B shows a plot of the difference between the $\gamma = 0$ and $\gamma = 1$ data to show this more clearly and here we can see that the scale is preferentially increasing the dispersion of the mid-expressed transcripts that formerly had negligible dispersion; examine the grey line of best fit (overlaid by the red line) for the trend. Panel B also shows the trend of the expression-dispersion relationship for transcripts that are classed as statistically significant. The red line shows the trendline with no added scale, and this trendline exactly overlays with the grey trendline of the bulk of transcripts. The

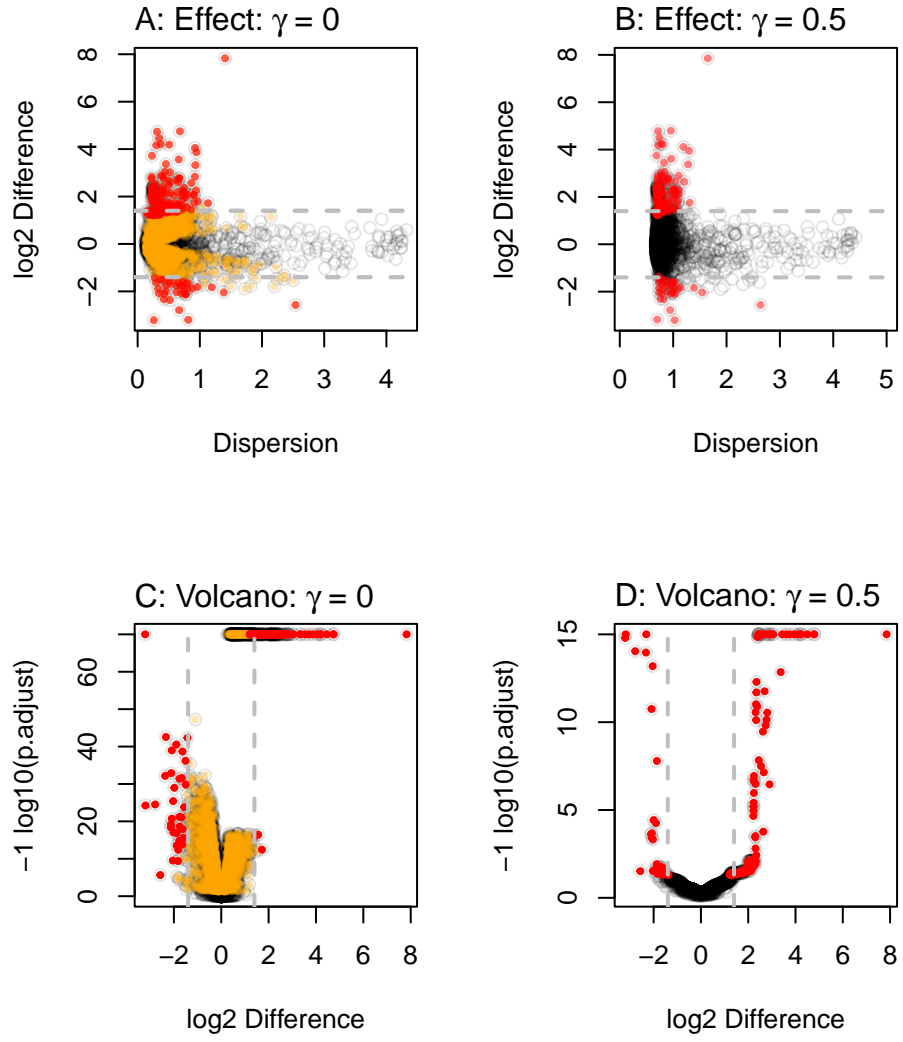


Figure 1: Effect and volcano plots for unscaled and scaled transcriptome analysis. ALDEX2 was used to conduct a differential abundance (DA) analysis on the yeast transcriptome dataset. The results were plotted to show the relationship between difference and dispersion using effect plots (A,B) or difference and the Benjamini-Hochberg corrected p-values (volcano plot C,D). Panels A,C are for the unscaled analysis, and Panels B,D are for the scaled analysis. Each point represents the values for one transcript, with the color indicating if that transcript was significant in the scaled analysis and unscaled analysis (red) or in the unscaled analysis only (orange). Points in grey are not statistically significantly different with any analysis. The horizontal dashed lines represent a $\log_2(\text{difference})$ of ± 1.4 .

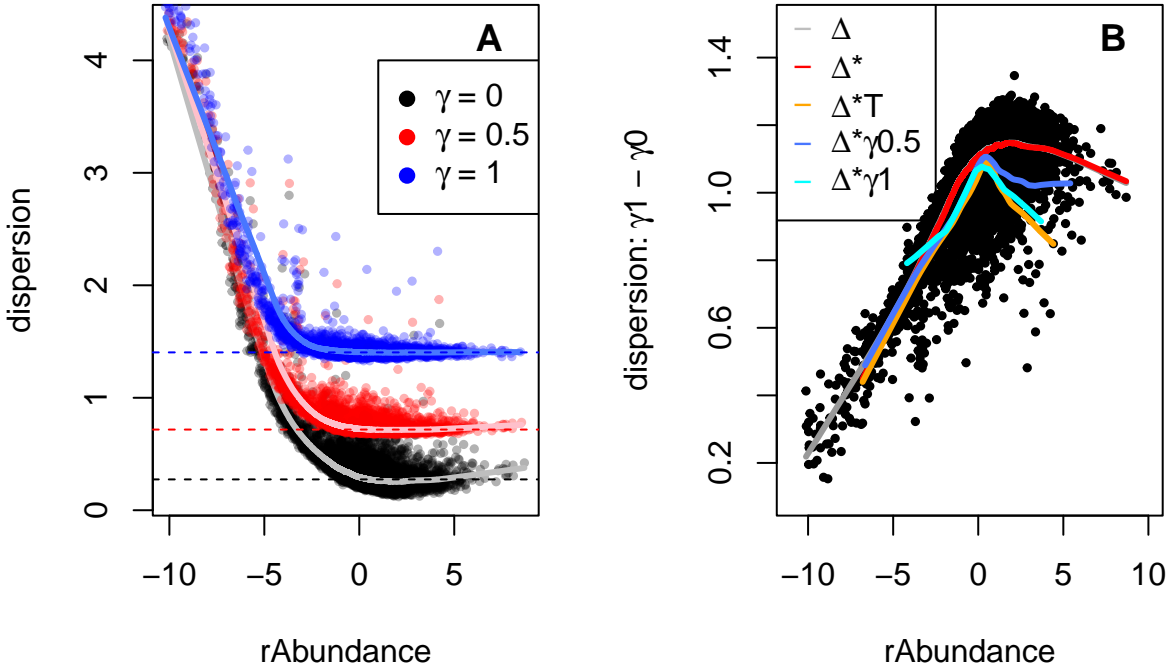


Figure 2: Adding scale uncertainty changes the dispersion distribution. Panel A shows a plot of the expected value for relative abundance vs the expected value for the pooled dispersion as output by `aldex.effect`. The dashed horizontal lines show the median value for the features with a rAbundance between -0.5 and 0.5, and the light colored lines are lowess lines of fit through the center of mass of the data. Panel B plots the dispersion difference between $\gamma = 1$ and $\gamma = 0$; note the non-linear relationship that highlights the rotation that is evident in Panel A. The colored lines indicate the lowess line of fit through the centre of mass of the plot for the various populations of points. The grey line is the total population and shows the difference Δ , the red line is the population of significant transcripts (*) with no scale, the orange line is the population of significant transcripts with a difference threshold (T) of about $\pm 2^{1.4}$ -fold change, the blue line is the population of significant transcripts with $\gamma = 0.5$, and the cyan line is the significant population with $\gamma = 1$. Δ : Difference, *: significant, T: thresholded.

orange trendline indicates those transcripts that are both statistically significant and that have a thresholded expression level of ± 1.4 , and the dark blue and cyan lines show the statistically significant trendline for $\gamma = 0.5$, or 1.0. Note that this has the effect of changing the distribution of parts identified as significant and that the substantially fewer significantly different genes are in the very high abundance but low dispersion category.

Housekeeping genes can be used to guide scale model choices.

Dos Santos et al. (46) used a vaginal metatranscriptome dataset to compare the gene expression in bacteria collected from healthy (H) and bacterial vaginosis (BV) affected women. In this environment, both the relative abundance of species between groups and the gene expression level within a species is different (47). Additionally, prior research suggests that the total number of bacteria is about 10 times more in the BV than in the H condition (18). Thus, this is an extremely challenging environment in which to determine differential abundance as there are both compositional and scale changes between conditions. The usual method to analyze vaginal metratranscriptome data is on a taxon-by-taxon basis (47–49) because the scale confounding can be ignored. Attempts at system-wide analysis show that many housekeeping functions are returned as differentially abundant between groups; a result likely due to a disconnect between the scale assumptions of the normalization used (7).

In this example, we show how to specify a user-defined, or *informed*, scale model explicitly that can account for some of these modeling difficulties. An informed scale model can control for both the mean difference of scale between groups (e.g., directly incorporate information on the differences in total number of bacteria between the BV and H conditions) as well as the uncertainty assumed in that difference. To specify a user-defined scale model, we can pass a matrix of scale values instead of a single estimate of gamma to `aldex.clr()`. This matrix should have the same number of rows as the of Monte-Carlo Dirichlet samples, and the same number of columns as the number of samples. While this matrix can be computed from scratch by the analyst, there is an `aldex.makeScaleModel()` function that can be used to simplify this step in most cases. This encodes the scale model as $\Lambda \sim N(\log 2\mu_n, \gamma^2)$, where μ_n represents the actual scale value for each sample. This can be a measured value (cell count, nucleic acid input, etc), or an imputed value. Nixon et al. (9) showed that only the ratio between the scale values for each sample was important; see Supplementary Figures 4 and 5 for a demonstration of this point.

Figure 3A shows an effect plot of the data where reads are grouped by function, corresponding to grouping homologous sequences regardless of the organism of origin. Each point represents one of 3728 KEGG functions (50). There are many more functions represented in the BV group (bottom) than in the healthy group (top). This is because the *Lactobacilli* that dominate a healthy vaginal microbiome have reduced genome content relative to the anaerobic organisms that dominate in BV, because there is a greater diversity of organisms in BV than in H samples, and because the BV condition has at least an order of magnitude more bacteria than does the H condition.

There are 101 functions with low dispersion that appear to be shared by both groups (boxed area in Figure 3A, and colored in cyan). Inspection shows that these largely correspond to core metabolic functions such as transcription, translation, ribosomal proteins, glycolysis, replication, chaperones, etc (Supplementary file `housekeeping.txt`). The transcripts of many of these are commonly used as invariant reference sequences (44) and so would not be expected to contribute to differences in ecosystem behaviour and should be centred on 0 difference. These should not be scored as among the most differentially abundant. The major group of these housekeeping functions is located off the line of no difference (being approximately located at $+1.5$). While changes in the abundance of housekeeping functions is a useful proxy for relative abundance of species in the environment, they tell us nothing about the functional capacity of the two groups as these are common to every organism. Of more interest is determining the functions that are different between groups because these are unique or over-expressed in one group relative to the other.

Applying the default scale model of $\gamma = 0.5$ increases the dispersion as expected but does little to move the large number of housekeeping functions toward the midline of no difference. This is as expected; the mean of the default scale model is based on the CLR normalization so no shift in location would be expected over the original ALDEEx2 model. Nevertheless, about 30% of the housekeeping functions are no longer statistically

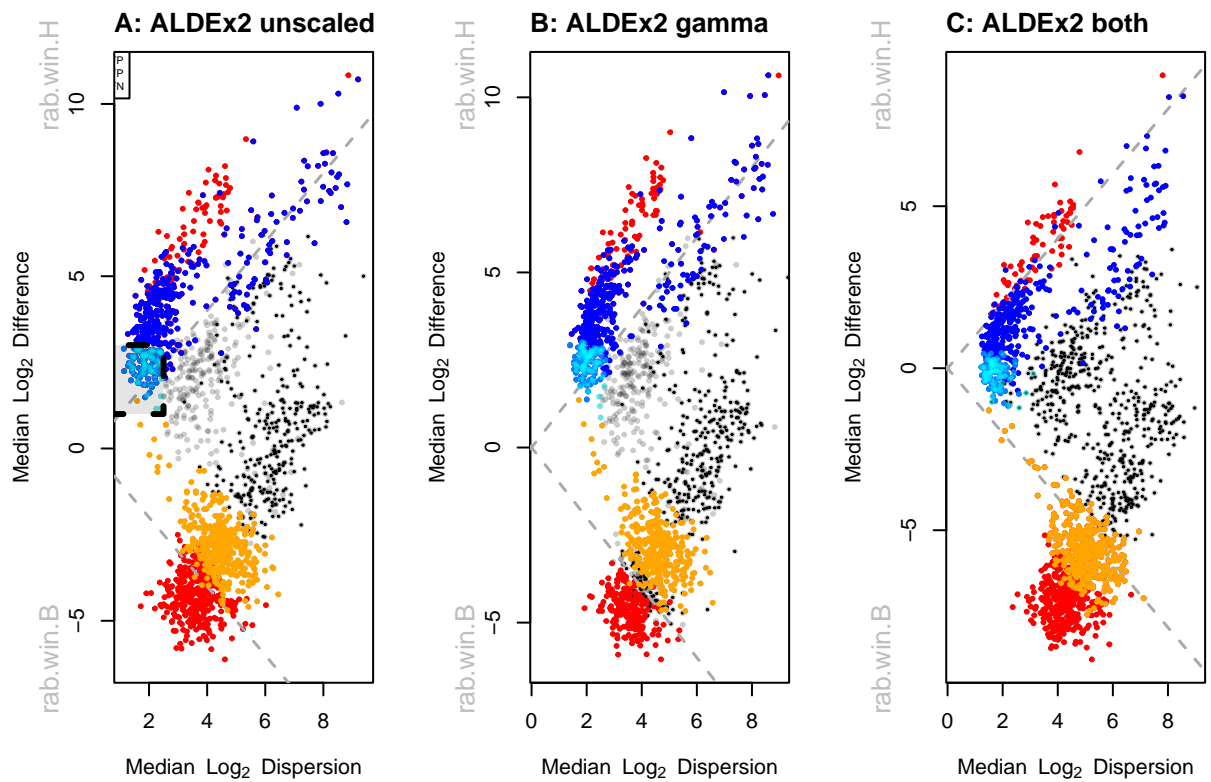


Figure 3: Analysis of vaginal transcriptome data aggregated at the Kegg Orthology (KO) functional level. Panel A shows an effect plot for the default analysis where the functions that are elevated in the healthy individuals have positive values and functions that are elevated in BV have negative values. Highlighted in the box are KOs that are almost exclusively housekeeping functions and are colored cyan. These housekeeping functions should be located on the midline of no difference. Panel B shows the same data scaled with $\gamma = 0.5$, which increase the minimum dispersion as before. Panel C shows the same data scaled with $\gamma = 0.5$ and a 0.15 fold difference in dispersion applied to the BV samples relative to the H samples. In these plots statistically significant ($FDR < 0.01$) functions in the informed model are in red, false positive functions are in blue, non-significant functions in black and false negative functions are in orange.

significantly different. Note that this change is simple to conduct, has no additional computational complexity and requires only a slight modification from the analyst.

Up to this point, scale uncertainty has been applied as an extension of the CLR normalization via the default scale model, but a user-defined scale adjustment can be applied to each condition, or even each sample independently through a custom scale matrix. Our starting point for this is to identify the naive scale estimate from the data, and this can be done by calculating the mean scale value for each group. The scale estimate for samples can be accessed in the `@scaleSamps` slot from the `aldex.clr` output. In this dataset the scale estimate for the healthy group is 17.41 and for the BV group is 14.59 for a difference of 2.82. This is interpreted as the scale of the H group of samples being 7.06 greater than the BV group and this precise but incorrect estimate places the location of the housekeeping genes off the midline of no difference.

We desire a scale model that approximately centres the housekeeping functions. We anticipate that housekeeping functions should be nearly invariant and so an appropriate scale in this dataset is likely closer to 0 than the naive estimate. While a user-defined scale model can be quite flexible with relative scales that are distinct for each group (or even each sample) along with their uncertainties, here we focus on using the `aldex.makeScaleMatrix()` function. This function uses a logNormal distribution to build a scale matrix given a user-specified mean difference between groups and uncertainty level. Applying a per-group relative differential scale of 0.15 moves the housekeeping functions to the midline of no difference (Figure 3C), and applying a gamma of 0.5 provides the same dispersion as in panel B). Note that now a significant number of functions are differentially up in BV that were formerly classed as not different without the full scale model (orange), or when only a default scale was applied. Inspection of the functions shows that these are largely missing from the *Lactobacillus* species and so should actually be captured as differentially abundant in the BV group. Thus, applying a differential scale allows us to distinguish between both false positives (housekeeping functions in cyan, and others in blue) and false negatives (orange functions) even in a very difficult to analyze dataset. The remarkable improvements in biological interpretation afforded by this full scale model, and the transferrability of it between sample cohorts of the same condition is outlined elsewhere (46). We suggest that the default scale model is sufficient when the data are approximately centred. However, an informed model is more appropriate with datasets are not well centred or when the investigator has prior information about the underlying biology.

Discussion

Biological systems are both predictably variable and stochastic (45) and current measurement methods that rely on high throughput sequencing fail to capture all of that variation, particularly variation due to scale (8, 9). In the absence of external information (such as spike-in probes (14), cell counting (1), FISH (51) etc) sequencing depth normalisation methods cannot recapture the scale information (14), and can only normalize for the technical variation due to sequencing depth.

Many groups have conducted benchmarking studies on different tools and normalizations used for the analysis of datasets such as transcriptomes(4, 21, 35, 37, 41) and microbiomes (3, 23, 24, 32, 34, 52). Generically, it is observed that the actual agreement between analysis methods can be modest, and no single method outperforms all others in every dataset or type of experiment. That different tools appear to work more reliably in different datasets from different sources can be explained as different normalizations being a better fit to the scale of a particular dataset by chance.

In the analysis of HTS data it is often observed that larger datasets converge on the majority of parts being significantly different (8, 35, 37), and that different analytic approaches result in different parts being chosen as significantly different (4, 24, 37, 41). Li et al. (35) conducted a permutation-based benchmarking study and found that popular tools performed worse than simple Wilcoxon rank-sum tests in controlling the FDR when sample sizes became large. They suggested that the presence of outliers were one of the factors driving this observation. Brooks et al. (53) suggested that inappropriate choice of benchmarking methods are also a major contributing factor. From our perspective, the disagreement between tools can be explained by the partially identifiable nature of the data; that is, the observed data are consistent with multiple ways of

estimating the parameters (8). Partially identifiable data exhibit multiple pathologies, chief among them being that different analytic approaches can produce different parameter estimates and that more data produces worse estimates because the additional data increases the precision of a flawed estimate (54).

Scale simulation is now built into ALDEx2 to address the issue of partially identifiability, and through this lens the two main root causes to common HTS data pathologies can be proposed. The first contributing factor is the observed very low dispersion estimate for many features that is a by-product of experimental design, sequencing and normalization. In the Schurch et al. (37) dataset, the data were from single colonies derived from a single culture. Thus, it is more accurate to describe the 96 samples as wet-lab technical replicates rather than independent samples. However, this type of replication approach is standard in the molecular literature, and would be expected to result in the very low dispersion that is observed.

In the yeast transcriptome dataset, applying the default scale model with $\gamma = 0.5$ a large number of transcripts with near 0 dispersion have had their dispersion increased (Figure 1D), and this results in modest number of transcripts, 205, being called significantly different as shown in the volcano plot in Figure 1D (red points). In addition, there was now a strong concordance between the difference and p-values (Figure 1D), this is not surprising. In hindsight, what is not obvious is why the unscaled volcano plot shows such poor correspondence. We suggest that this can be explained by random fluctuations in the many variance estimates with very low values, and this is supported by the plot shown in Figure 2B. Furthermore, overplotting the significant transcripts identified after adding scale uncertainty on the un-scaled analysis shows that adding scale uncertainty removes the need for the dual cutoff. Indeed, adding scale uncertainty reduces the significant transcripts to a subset of those identified with the dual cutoff that have the largest effect size. Thus, incorporating scale uncertainty through the default scale model allows us to determine which variables are likely to be significant due to sequencing and normalization, and which are significantly different even with scale uncertainty included.

While the actual scale of the underlying environment is inaccessible post-sequencing, we can study the sensitivity of the results to the choice of normalization and thus scale. Varying amounts of scale uncertainty is incorporated using the `gamma` parameter that controls the amount uncertainty added to the CLR mean assumption when we call either `aldex()`, or `aldex.clr()`. The ALDEx2 package contains a sensitivity analysis function, `aldex.senAnalysis()`, that can be used to explore the effect of different amounts of scale uncertainty, and an example is shown in Supplementary Figure 2 for the yeast transcriptome dataset. Here it is clear that even tiny amounts of scale preclude the majority of transcripts from being considered statistically significant. In practice, we suggest that a `gamma` parameter between 0.5 and 1 is realistic for most experimental designs, but further work is needed.

The second contributing factor is unacknowledged asymmetry in many datasets. In the case of asymmetry, the use of a user-specified scale model can be very useful for otherwise difficult-to-analyze datasets such as meta-transcriptomes and in-vitro selection datasets where the majority of features can change. We showed one such example for the metatranscriptome dataset in Figure 3. Here the dataset was highly asymmetrical, and the TMM and RLE normalizations could not fully move all the housekeeping genes to the midline of no difference or the tools exhibited other pathologies (Supplemental Figure 6). Incorporating differential scale on a per-group basis moves the mass of the housekeeping functions towards the midline of no difference and so affects both Type I and Type II error rates. It is also of note that in the case of true biological replicates (different individuals) that adding a modest amount of scale $\gamma = 0.5$ had little effect on the concordance between the difference between groups and the p-values as shown in Supplementary Figure 7. Thus, in this dataset the scale mis-specification was affecting mainly the location of the difference between groups.

In the metatranscriptome analysis, transcripts that were previously not classed as differentially abundant were now called as significantly different, and the housekeeping transcripts move from being significantly different to not being identified as such. Note the assumption that housekeeping genes should not generally be included in differential abundance analysis is implicit in the dual p-value:fold-change cutoff approach in widespread use. While we acknowledge that some prior information on which housekeeping transcripts should not be classed as differentially abundant is needed, we suggest that this information is widely available and is already used when performing the gold-standard quantitative PCR test of differential abundance (55, 56). Thus, the use of this prior knowledge is not unique to our approach.

Beyond concerns of fidelity and rigor, scale models also enhance the reproducibility and transparency of HTS analyses. The addition of scale uncertainty essentially tests the model over a range of normalizations (8) and so can replace the consensus approach that has been proposed by some groups (24, 57) with no additional computational overhead. Thus, an advantage of incorporating scale is that analyses can be made much more robust such that actual or potential differences in scale can be tested and accounted for explicitly. This occurs because rather than using an implicit assumption (e.g., $\log \mathbf{W}^\perp = 1/G_n$ for the CLR normalization), scale models can make this an explicit part of the model building process. While it is beyond the scope of the present article, we note that there are many ways of building scale models that enhance the interpretability of the parameters and assumptions and a detailed description of these points is describe elsewhere (8). In this work, we simply use the parameter γ in the default scale model as a term that represents uncertainty in the CLR assumption and note that larger values of γ correspond to more uncertainty in this assumption. In the metatranscriptome example and elsewhere (9), we also show that the ratio of scales between conditions can be used to build a full scale model when the conditions have dramatically different underlying scales.

The ALDEx2 R package is readily amenable for incorporating scale uncertainty. Originally, this tool used the only the Dirichlet distribution to sample compositional uncertainty, but scale uncertainty can be added through the use of a scale model with no additional computational complexity. By default, ALDEx2 samples scale from a logNormal distribution inspired by the CLR normalization. However, scale uncertainty can be sampled from any distribution depending on prior knowledge or preference, using the option to introduce a full informed scale model that encapsulates both uncertainty and asymmetry in underlying scale.

In summary, we supply a toolkit that makes incorporating scale simple to incorporate for any type of HTS dataset. While the underlying scale of the system is generally inaccessible, the effect of scale on the analysis outcomes can be modelled and can help explain some of the underlying biology, and known issues with the analysis of HTS data. Adding scale information to the analysis allows for more robust inference because the features that are sensitive to scale can be identified and their impact on conclusions weighted accordingly. Additionally, the use of user-defined scale models permits difficult to analyze datasets to be examined in a robust and principled manner even when the majority of features are asymmetrically distributed or expressed (or both) in the groups (46). Thus, reporting scale uncertainty should become a standard practice in the analysis of HTS datasets as a way to identify which features are most robust to differences in the underlying system.

References

1. Vandeputte,D., Kathagen,G., D'hoe,K., Vieira-Silva,S., Valles-Colomer,M., Sabino,J., Wang,J., Tito,R.Y., De Commer,L., Darzi,Y., *et al.* (2017) Quantitative microbiome profiling links gut community variation to microbial load. *Nature*, **551**, 507–511.
2. Props,R., Kerckhof,F.-M., Rubbens,P., De Vrieze,J., Hernandez Sanabria,E., Waegeman,W., Monsieurs,P., Hammes,F. and Boon,N. (2017) Absolute quantification of microbial taxon abundances. *ISME J*, **11**, 584–587.
3. Thorsen,J., Brejnrod,A., Mortensen,M., Rasmussen,M.A., Stokholm,J., Al-Soud,W.A., Sørensen,S., Bisgaard,H. and Waage,J. (2016) Large-scale benchmarking reveals false discoveries and count transformation sensitivity in 16S rRNA gene amplicon data analysis methods used in microbiome studies. *Microbiome*, **4**, 62.
4. Quinn,T.P., Crowley,T.M. and Richardson,M.F. (2018) Benchmarking differential expression analysis tools for RNA-seq: Normalization-based vs. Log-ratio transformation-based methods. *BMC Bioinformatics*, **19**, 274.
5. Zhang,S. and Cao,J. (2009) A close examination of double filtering with fold change and t test in microarray analysis. *BMC Bioinformatics*, **10**, 402.

6. Ebrahimpoor,M. and Goeman,J.J. (2021) Inflated false discovery rate due to volcano plots: Problem and solutions. *Brief Bioinform*, **22**.
7. Wu,J.R., Macklaim,J.M., Genge,B.L. and Gloor,G.B. (2021) Finding the centre: Compositional asymmetry in high-throughput sequencing datasets. In Filzmoser,P., Hron,K., Martì-Fernàndez,J.A., Palarea-Albaladejo,J. (eds), *Advances in compositional data analysis: Festschrift in honour of vera pawlowsky-glahn*. Springer International Publishing, Cham, pp. 329–346.
8. Nixon,M.P., Letourneau,J., David,L.A., Lazar,N.A., Mukherjee,S. and Silverman,J.D. (2023) Scale reliant inference.
9. Nixon,M.P., Gloor,G.B. and Silverman,J.D. (2024) Beyond normalization: Incorporating scale uncertainty in microbiome and gene expression analysis. *bioRxiv*, 10.1101/2024.04.01.587602.
10. Lovell,D., Müller,W., Taylor,J., Zwart,A. and Helliwell,C. (2011) Proportions, percentages, ppm: Do the molecular biosciences treat compositional data right? In Pawlowsky-Glahn,V., Buccianti,A. (eds), *Compositional Data Analysis: Theory and Applications*. John Wiley; Sons New York, NY, London, pp. 193–207.
11. Quinn,T.P., Erb,I., Gloor,G., Notredame,C., Richardson,M.F. and Crowley,T.M. (2019) A field guide for the compositional analysis of any-omics data. *Gigascience*, **8**.
12. Lovell,D., Pawlowsky-Glahn,V., Egoscue,J.J., Marguerat,S. and Bähler,J. (2015) Proportionality: A valid alternative to correlation for relative data. *PLoS Comput Biol*, **11**, e1004075.
13. Nie,Z., Hu,G., Wei,G., Cui,K., Yamane,A., Resch,W., Wang,R., Green,D.R., Tessarollo,L., Casellas,R., et al. (2012) C-Myc is a universal amplifier of expressed genes in lymphocytes and embryonic stem cells. *Cell*, **151**, 68–79.
14. Lovén,J., Orlando,D.A., Sigova,A.A., Lin,C.Y., Rahl,P.B., Burge,C.B., Levens,D.L., Lee,T.I. and Young,R.A. (2012) Revisiting global gene expression analysis. *Cell*, **151**, 476–82.
15. Scott,M., Gunderson,C.W., Mateescu,E.M., Zhang,Z. and Hwa,T. (2010) Interdependence of cell growth and gene expression: Origins and consequences. *Science*, **330**, 1099–102.
16. Yoshikawa,K., Tanaka,T., Ida,Y., Furusawa,C., Hirasawa,T. and Shimizu,H. (2011) Comprehensive phenotypic analysis of single-gene deletion and overexpression strains of *saccharomyces cerevisiae*. *Yeast*, **28**, 349–61.
17. Lin,J. and Amir,A. (2018) Homeostasis of protein and mRNA concentrations in growing cells. *Nat Commun*, **9**, 4496.
18. Zozaya-Hinchliffe,M., Lillis,R., Martin,D.H. and Ferris,M.J. (2010) Quantitative PCR assessments of bacterial species in women with and without bacterial vaginosis. *J Clin Microbiol*, **48**, 1812–9.
19. Ravel,J., Gajer,P., Abdo,Z., Schneider,G.M., Koenig,S.S.K., McCulle,S.L., Karlebach,S., Gorle,R., Russell,J., Tacket,C.O., et al. (2011) Vaginal microbiome of reproductive-age women. *Proc Natl Acad Sci U S A*, doi/10.1073/pnas.100611107.
20. Hummelen,R., Fernandes,A.D., Macklaim,J.M., Dickson,R.J., Changalucha,J., Gloor,G.B. and Reid,G. (2010) Deep sequencing of the vaginal microbiota of women with HIV. *PLoS One*, **5**, e12078.
21. Bullard,J.H., Purdom,E., Hansen,K.D. and Dudoit,S. (2010) Evaluation of statistical methods for normalization and differential expression in mRNA-seq experiments. *BMC Bioinformatics*, **11**, 94.

22. Dillies,M.-A., Rau,A., Aubert,J., Hennequet-Antier,C., Jeanmougin,M., Servant,N., Keime,C., Marot,G., Castel,D., Estelle,J., *et al.* (2013) A comprehensive evaluation of normalization methods for Illumina high-throughput RNA sequencing data analysis. *Brief Bioinform*, **14**, 671–83.
23. Weiss,S., Xu,Z.Z., Peddada,S., Amir,A., Bittinger,K., Gonzalez,A., Lozupone,C., Zaneveld,J.R., Vázquez-Baeza,Y., Birmingham,A., *et al.* (2017) Normalization and microbial differential abundance strategies depend upon data characteristics. *Microbiome*, **5**, 27.
24. Nearing,J.T., Douglas,G.M., Hayes,M.G., MacDonald,J., Desai,D.K., Allward,N., Jones,C.M.A., Wright,R.J., Dhanani,A.S., Comeau,A.M., *et al.* (2022) Microbiome differential abundance methods produce different results across 38 datasets. *Nat Commun*, **13**, 342.
25. Hughes,J.B. and Hellmann,J.J. (2005) The application of rarefaction techniques to molecular inventories of microbial diversity. *Methods Enzymol*, **397**, 292–308.
26. Mortazavi,A., Williams,B.A., McCue,K., Schaeffer,L. and Wold,B. (2008) Mapping and quantifying mammalian transcriptomes by RNA-seq. *Nat Methods*, **5**, 621–8.
27. Wagner,G.P., Kin,K. and Lynch,V.J. (2012) Measurement of mRNA abundance using RNA-seq data: RPKM measure is inconsistent among samples. *Theory Biosci*, **131**, 281–5.
28. Robinson,M.D. and Oshlack,A. (2010) A scaling normalization method for differential expression analysis of RNA-seq data. *Genome Biol*, **11**, R25.1–R25.9.
29. Aitchison,J. (1982) The statistical analysis of compositional data. *Journal of the Royal Statistical Society: Series B (Methodological)*, **44**, 139–160.
30. Anders,S. and Huber,W. (2010) Differential expression analysis for sequence count data. *Genome Biol*, **11**, R106.
31. Fernandes,A.D., Macklaim,J.M., Linn,T.G., Reid,G. and Gloor,G.B. (2013) ANOVA-like differential expression (ALDEx) analysis for mixed population RNA-seq. *PLoS One*, **8**, e67019.
32. Yerke,A., Fry Brumit,D. and Fodor,A.A. (2024) Proportion-based normalizations outperform compositional data transformations in machine learning applications. *Microbiome*, **12**, 45.
33. Fernandes,A.D., Reid,J.N., Macklaim,J.M., McMurrrough,T.A., Edgell,D.R. and Gloor,G.B. (2014) Unifying the analysis of high-throughput sequencing datasets: Characterizing RNA-seq, 16S rRNA gene sequencing and selective growth experiments by compositional data analysis. *Microbiome*, **2**, 15.1–15.13.
34. Hawinkel,S., Mattiello,F., Bijnens,L. and Thas,O. (2018) A broken promise : Microbiome differential abundance methods do not control the false discovery rate. *BRIEFINGS IN BIOINFORMATICS*.
35. Li,Y., Ge,X., Peng,F., Li,W. and Li,J.J. (2022) Exaggerated false positives by popular differential expression methods when analyzing human population samples. *Genome Biol*, **23**, 79.
36. Cui,X. and Churchill,G.A. (2003) Statistical tests for differential expression in cDNA microarray experiments. *Genome Biol*, **4**, 210.1–210.10.
37. Schurch,N.J., Schofield,P., Gierliński,M., Cole,C., Sherstnev,A., Singh,V., Wrobel,N., Gharbi,K., Simpson,G.G., Owen-Hughes,T., *et al.* (2016) How many biological replicates are needed in an RNA-seq experiment and which differential expression tool should you use? *RNA*, **22**, 839–51.
38. Gierliński,M., Cole,C., Schofield,P., Schurch,N.J., Sherstnev,A., Singh,V., Wrobel,N., Gharbi,K., Simp-

- son,G., Owen-Hughes,T., *et al.* (2015) Statistical models for RNA-seq data derived from a two-condition 48-replicate experiment. *Bioinformatics*, **31**, 3625–3630.
39. Halsey,L.G., Curran-Everett,D., Vowler,S.L. and Drummond,G.B. (2015) The fickle p value generates irreproducible results. *Nat Methods*, **12**, 179–85.
 40. Benjamini,Y. and Hochberg,Y. (1995) Controlling the false discovery rate: A practical and powerful approach to multiple testing. *Journal of the Royal Statistical Society. Series B (Methodological)*, **57**, 289–300.
 41. Soneson,C. and Delorenzi,M. (2013) A comparison of methods for differential expression analysis of RNA-seq data. *BMC Bioinformatics*, **14**, 91.
 42. Maza,E., Frasse,P., Senin,P., Bouzayen,M. and Zouine,M. (2013) Comparison of normalization methods for differential gene expression analysis in RNA-seq experiments: A matter of relative size of studied transcriptomes. *Commun Integr Biol*, **6**, e25849.
 43. Gloor,G., Macklaim,J. and Fernandes,A. (2016) Displaying variation in large datasets: Plotting a visual summary of effect sizes. *Journal of Computational and Graphical Statistics*, **25**, 971–979.
 44. Rocha,D.J.P.G., Castro,T.L.P., Aguiar,E.R.G.R. and Pacheco,L.G.C. (2020) Gene expression analysis in bacteria by RT-qPCR. *Methods Mol Biol*, **2065**, 119–137.
 45. Taniguchi,Y., Choi,P.J., Li,G.-W., Chen,H., Babu,M., Hearn,J., Emili,A. and Xie,X.S. (2010) Quantifying e. Coli proteome and transcriptome with single-molecule sensitivity in single cells. *Science*, **329**, 533–8.
 46. Dos Dos Santos,S.J., Copeland,C., Macklaim,J.M., Reid,G. and Gloor,G.B. (2024) Vaginal metatranscriptome meta-analysis reveals functional BV subgroups and novel colonisation strategies. *bioRxiv*, 10.1101/2024.04.24.590967.
 47. Macklaim,J.M., Fernandes,A.D., Di Bella,J.M., Hammond,J.-A., Reid,G. and Gloor,G.B. (2013) Comparative meta-RNA-seq of the vaginal microbiota and differential expression by lactobacillus iners in health and dysbiosis. *Microbiome*, **1**, 12.
 48. Deng,Z.-L., Gottschick,C., Bhuju,S., Masur,C., Abels,C. and Wagner-Döbler,I. (2018) Metatranscriptome analysis of the vaginal microbiota reveals potential mechanisms for protection against metronidazole in bacterial vaginosis. *mSphere*, **3**.
 49. Fettweis,J.M., Serrano,M.G., Brooks,J.P., Edwards,D.J., Girerd,P.H., Parikh,H.I., Huang,B., Arodz,T.J., Edupuganti,L., Glascock,A.L., *et al.* (2019) The vaginal microbiome and preterm birth. *Nat Med*, **25**, 1012–1021.
 50. Okuda,S., Yamada,T., Hamajima,M., Itoh,M., Katayama,T., Bork,P., Goto,S. and Kanehisa,M. (2008) KEGG atlas mapping for global analysis of metabolic pathways. *Nucleic Acids Res*, **36**, W423–6.
 51. Marguerat,S., Schmidt,A., Codlin,S., Chen,W., Aebersold,R. and Bähler,J. (2012) Quantitative analysis of fission yeast transcriptomes and proteomes in proliferating and quiescent cells. *Cell*, **151**, 671–83.
 52. McMurdie,P.J. and Holmes,S. (2014) Waste not, want not: Why rarefying microbiome data is inadmissible. *PLoS Comput Biol*, **10**, e1003531.
 53. Brooks,T.G., Lahens,N.F., Mrčela,A. and Grant,G.R. (2024) Challenges and best practices in omics benchmarking. *Nat Rev Genet*, **25**, 326–339.

54. Gustafson,P. (2015) Bayesian inference for partially identified models: Exploring the limits of limited data CRC Press.
55. Thellin,O., Zorzi,W., Lakaye,B., De Borman,B., Coumans,B., Hennen,G., Grisar,T., Igout,A. and Heinen,E. (1999) Housekeeping genes as internal standards: Use and limits. *J Biotechnol*, **75**, 291–5.
56. SEQC/MAQC-III Consortium (2014) A comprehensive assessment of RNA-seq accuracy, reproducibility and information content by the sequencing quality control consortium. *Nat Biotechnol*, **32**, 903–14.
57. Song,H., Ling,W., Zhao,N., Plantinga,A.M., Broedlow,C.A., Klatt,N.R., Hensley-McBain,T. and Wu,M.C. (2023) Accommodating multiple potential normalizations in microbiome associations studies. *BMC Bioinformatics*, **24**, 22.